Communication in Physical Sciences, 2023, 9(4): 453-464

Investigation of Snail shells as an Adsorbent and Precursor for the synthesis of Calcium Oxide Nanoparticles for the Removal of Amoxicillin from Aqueous Solution

Ubong Ime Essien*, Anduang O. Odiongenyi, Clement O. Obadimu, Iniobong S. Enengedi,
Received: 15 June 2023/Accepted 08 August 2023/Published 18 August 2023

Abstract: *Snail shells are rich in $CaCO_3$ as its major constituent. Consequently, its application for the adsorption removal of contaminants has been linked to the presence of this compound. In this study, comparative efforts were made to adopt snail shells in a direct and indirect approach toward the adsorption removal of amoxicillin from an aqueous solution. The direct approach was implemented by using the powder samples obtained from crushing the snail shells. The indirect method was centred on resource recovery technology, which involved the fabrication of calcium nanoparticles from the crushed powdered sample. Both sets of adsorbents were candidates for the batch adsorption removal of amoxicillin from water. The adsorption removal efficiency by the nanoparticles showed an outstanding gap regarding their performance compared to the crude samples. However, adsorption in all cases was influenced by temperature, concentration of the drug, ionic strength, time and pH. The pseudo-second order, intraparticle diffusion and liquid diffusion showed favourable fits to the experimental data while the thermodynamic values showed exothermic adsorption for the nanoparticles and endothermic for the crude sample. The adsorption behaviours of both adsorbents displayed excellent fitness for the Langmuir model. Based on the results of the study, Nanoparticles obtained from snail shells have better adsorption properties than the crude samples due to enhanced surface properties.*

Keywords: *Resource recovery, snail shells, calcium oxide nanoparticles, remediation, amoxicillin*

Ubong Ime Essien*
Department of Chemistry, Faculty of Physical Sciences, Akwa Ibom State University, Mkpat Enin, P. M. B. 1167, Uyo, Nigeria,
Email: ubongesin@gmail.com*

Anduang O. Odiongenyi
Department of Chemistry, Faculty of Physical Sciences, Akwa Ibom State University, Mkpat Enin, P. M. B. 1167, Uyo, Nigeria
Email: anduangodiongenyi@aksu.edu.ng
Orcid id: https://orcid.org/0000-0002-6842-9976

Clement O. Obadimu
Department of Chemistry, Faculty of Physical Sciences, Akwa Ibom State University, Mkpat Enin, P. M. B. 1167, Uyo, Nigeria
Email: lementobadimu@gmail.com

Iniobong S. Enengedi
Department of Chemistry, Faculty of Physical Sciences, Akwa Ibom State University, Mkpat Enin, P. M. B. 1167, Uyo, Nigeria
Email:, iniobongenengedi@aksu.edu.ng

1.0 Introduction

Waste management has a multi-dimensional approach but efficient waste management must fit into the design of providing the solution that will terminate waste or at least reduce the volume of the generated wastes to the level that the contamination of the environment is not significant (Zargar *et al*., 2023) . Solid wastes have some unique challenges, often aligned to

disposal management because of the volume such waste may occupy (Adedara *et al*., 2023)). In the management of non-biodegradable wastes, the most commendable technologies are re-use, recycling and resource recovery (Kofoworola, 2007). Crustacean shells are one of the non-biodegradable wastes in the environment, whose management must be given special consideration because they are non-biodegradable and can occupy large space in addition to the provision of hosting surfaces for other contaminants. However, because of adequate knowledge of their chemical constituents, which is majorly $CaCO_3$, adequate management systems have been achieved (Abubakar *et al*., 2022. One of such is the conversion to nanoparticles or nanocomposites, which are most needed in various aspects of life including engineering, environment, medicine, pharmaceutical, electronics, etc. (Bayuseno *et* al., 2022; Habte *et* al., 2019; Hamester *et al*., 2012). Snail shells are dominant in marine areas and the waste that can be recovered from this animal often outweighs the edible flesh. Literature reveals that these shells contain above 95-98% $CaCO_3$, indicating that it is a good precursor for the synthesis of calcium oxide nanoparticles (CaONPs) either by direct decomposition or by the sol-gel method (Ngouoko *et* al., 2022; Zuliantoni *et al*., 2022).

CaONPs have several interesting applications in the environmental industries, especially as adsorbents, filters, photocatalysts, fire repellants, etc (Jadhav *et al*., 2022; Kasirajan *et al*., 2022; Khie *et al*., 2022). The application of CaONPs as adsorbents have been widely reviewed and in almost all cases, they are graded as highly efficient adsorbent (Mostafa *et al*., 2022). Therefore, efforts to increase the rate of the production of these valuable materials can contribute significantly to the solutions to some problems, especially those associated with the environment. In this study, the management of snail waste through a resource recovery approach is proposed through the synthesis of CaONPs, which are also employed as an adsorbent for the removal of amoxicillin contaminants from water.

2.0 Materials and Methods

Snail shells were collected from a dumpsite in Ikot Ekpene town (Nigeria) where they are processed. The processing is done to remove the flesh from the shell. The shells were washed with hot distilled water, dried and crushed to fine powder using an electric milling machine. The crushed samples were dried to constant weight and preserved. Part of the finely powdered sample was preserved for direct application in the batch adsorption experiment while the remaining samples were used in the synthesis of nanoparticles;

The synthesis of calcium oxide nanoparticles (CaONPs) from snail shells relies on its dominant content of $CaCO_3$. The first stage in the synthesis involved the reaction of 100 g of the powdered snail sample with 2 M HCl solution. The reaction mixture was continuously stirred to enable the liberation of CO_2. The product of the reaction ($CaCl_2$) was allowed to dry and then washed severally with distilled water and re-dried. The $CaCl_2$ was made to react with 50% NaOH solution to produce $Ca(OH)_2$ which was dried and finally calcined at 700 °C.

The particle size analysis was done using the Brunauer-Emmett-Teller (BET) techniques (Nova4200e made in Japan) after obtaining data for nitrogen adsorption

Amoxicillin drugs were obtained from a pharmaceutical store in Ikot Ekpene and were used without further purification. Different concentrations of the drug (20, 40, 60, 80 and 100 ppm) were prepared from the prepared stock solution using distilled water for dilution. All measurements concerning concentrations were carried out using a UV visible spectrophotometer (V1. 63.0). The wavelength of maximum absorption by the drug was recorded as 272 nm after scanning over a long range. A calibration curve (Fig. 1) was also

prepared to ascertain the relationship between absorbance and the concentration of the drug

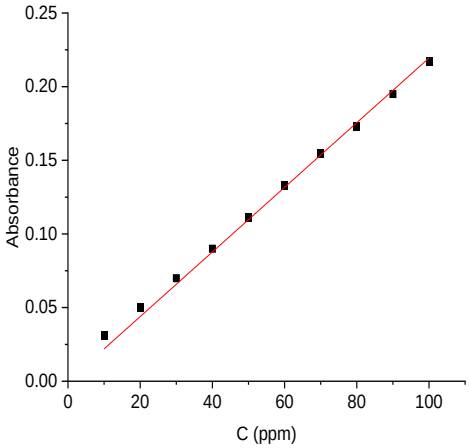

Fig. 1: Calibration curve for amoxicillin

The calibration curve presented a linear model with zero intercepts and an R^2 value of 0.9999 which confirmed that Beer-Lambert's law was obeyed for the drug. The evaluated slope value was 0.00219 while the error for the slope was 0.00002187. Consequently, all calculations from absorbance measurements were done using the obtained slope as the reference.

Bath adsorption experiment was carried out as reported widely in the literature (Akpaniudo and Chibuzo (2020; Odionegeyi, 2019, 2022). The equilibrium concentration of the drug adsorbed and the percentage amount of the drug removed were evaluated using equations 1 and 2 (Odiongenyi, 2010)

$$Q_e(mg/g) = \frac{C_0 - C_t}{m} \times \frac{V}{1} \quad (1)$$

$$\%\, Removal = \frac{C_0 - C_t}{C_0} \times \frac{100}{1} \quad (2)$$

In the above equations, C_0 and C_t are the initial and final concentrations respectively, m is the mass of the adsorbent and V is the volume of the solution of the adsorbate used for the study. Batch adsorption experiments were conducted to investigate the effect of concentration of the drug, time, pH, temperature and ionic strength. Each of the listed factors was investigated independently using a fixed concentration of the drug (i.e. 100 ppm) except in the investigation of the effect of the initial concentration of the drug, where the solution concentrations were varied.

3.0 Results and Discussion

3.1 Characterization of the adsorbate

The multi-Brunauer-Emmett-Teller (MBET) principle is based on equation 3 (Eddy *et al*., 2023a)

$$\frac{1}{N[(P_0/P)-1]} = \frac{1}{N_m} + \frac{C-1}{N_m C}\left(\frac{P}{P_0}\right) \quad (3)$$

where N is the amount of nitrogen gas adsorbed at a pressure, P, while N_m is the monolayer adsorption capacity, P_0 is the initial pressure, and C is a constant that is related to the heat capacity. $C = [q_{ads} - q_{cond}]/RT$. q_{ads} is the adsorption heat while q_{cond} is the heat of condensation of the adsorbate. In Fig. 1, the multi-point BET plots for the adsorption of nitrogen by the synthesized nanocomposite gave R^2 0.999. From the plot, the surface area was evaluated using equation 4 (Eddy *et al*., 2022b)

$$Mult - BET = \frac{1}{\frac{1}{X_m} + \frac{C-1}{X_m C}} * A \quad (4)$$

where A is the cross-sectional area of the adsorbate, which is approximately equal to 0.162, 0.189 and 0.201 m^2 for nitrogen adsorption on CaONPs from the bonnet, snail and clam shells. The evaluated multi-BET surface area for the nanocomposite was 824.33 m^2, which suggests an enhanced efficiency when compared to values reported by others for CaONPs synthesized from different sources as shown in Table 1. The particle size of the synthesized nanoparticles was evaluated from the DFT method as 11.22 nm, which is also compared with some literature values (Table 1)

3.2 Batch adsorption experiment

In Fig. 2, influences of concentration and period of contact on the percentage removal of amoxicillin from water are demonstrated graphically. The two plots reveal that the

nanoparticles generally show enhanced performance over the unprocessed snail samples. Concerning concentration, the percentage of amoxicillin removed by adsorption from the aqueous media decreases with an increase in concentration. This may be due to the complete occupancy of the active adsorption sites at a certain concentration, above which, the number of available sites for adsorption becomes limited, hence reducing adsorption efficiency for higher concentrations.

Table 1: Comparison of surface properties of CaONPs from different precursor

Precursor	BET surface area (m^2/g)	Pore diameter (nm)	Reference
Waste carbonation mud	747.62	15.00	Mostafa *et al*. (2023)
$Ca(OH)_2$	4.340	11.00	Khine *et al*. (2022)
Eggshell	77.40	24.34	Jalu *et al*. (2022)
Scotch Bonnet shells	785.02	2.65	Odiongenyi *et al*. (2023)
Industrial waste	134,80	50.00	Abdelatif *et al*. (2020)
Gigas shell	520.06	8.10	Eddy *et al*. (2022b)
Oyster shell	108.39	2.88	Ogoko *et al*. (2023)
$Ca(OH)_2$	71.49	12.45	Toamah and Fadhil (2019)

Maximum adsorption efficiency of the nanoparticles and the unprocessed snail shell powder were observed at a concentration of 10 ppm and the values were 96 and 76% approximately. The period of contact (Fig. 2) demonstrated a favourable influence on the adsorption removal of the drug sample for the aqueous system with the nanoparticles and unprocessed snail shell powder showing efficiencies of 98 and 86% respectively, which correlated with the enhancement of efficiency due to sufficient time needed to activate the available adsorption sites. The enhanced surface area of adsorption demonstrated by the nanoparticles over the raw materials confirms that the surface area of the nanoparticles is larger than that of the raw materials.

The pH of the aqueous media was also seen as an influencing factor for the adsorption removal of amoxicillin from aqueous solution and generally depicted a decrease in adsorption with an increase in pH, which suggests that the adsorption of amoxicillin is favoured by acidic pH (Fig. 3). Between the pH of 0 and 2.68, amoxicillin is positively charged but both are positively and negatively charged between the pH of 2. 68 and 7.49; but above the pH value of 7. 49, the drug is negatively charged (Novo *et al*., 2022). Most literature values indicate that the point at zero pH for calcium oxide nanoparticles is above 6.5 (Eddy *et al*., 20023a-b), which suggests that above this pH, the surface of the adsorbent would be negatively charged and will repel the adsorption of amoxicillin since the drug tend to be more negative as pH increases. Hence decrease in adsorption is justified by the effect of pH as observed in the plot (Fig. 3).

As with other factors, the nanoparticles showed enhanced performance as adsorbent over the raw powdered sample, which is due to a more uniformity of the nanoparticle over the raw sample. This disparity was more significant when the effect of temperature on the adsorption efficiency of the tested materials was considered (also shown in Fig, 3). The adsorbent from the crude sample demonstrated an unsteady trend compared to the uniform trend displayed by the nano adsorbent. This suggests that surface imperfection or instability might have contributed to the irregularity in the adsorption pattern of the crude samples.

Nanoparticles are known for their high stability (Odoemelam *et al*., 2023). Consequently, the nanoparticles showed higher adsorption efficiencies at all temperatures compared to the crude snail sample, which was numerically

equal to 89 and 62% respectively. The adsorption efficiency of the nanoparticles demonstrated progressive increment with temperature while that of the crude sample showed an irregular trend, probably due to the denature of the adsorption sites at higher temperatures.

Interestingly, both nano and crude samples showed a progressive rise in adsorption efficiency with ionic strength as indicated in Fig. 4. This is attributed to the synergistic enhancement of adsorption by the KCl (Eddy *et al*., 2022b).

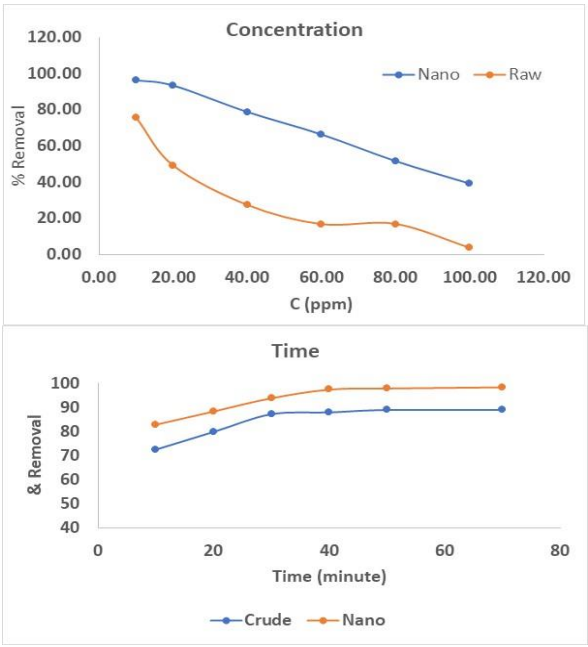

Fig. 2: Variation of percentage amoxicillin removed with concentration and time

3.3 Adsorption isotherm

Among the tested adsorption isotherm, the Langmuir isotherm gave the best fit for the removal of amoxicillin by CaONPs synthesized from snail shells (Condurache *et* al., 2022)

$$\frac{C_e}{Q_e} = \frac{1}{k_L Q_{max}} + \frac{C_e}{Q_{max}} \qquad (5)$$

Following the obedient of the adsorption data to the Langmuir model, a plot of $\frac{C_e}{Q_e}$ against C_e (Fig. 5) was observed to be linear and displayed an excellent degree of fitness based on the evaluated R^2 and error values shown in Table 2. It is confirmed from the results that a better Langmuir maximum adsorption capacity (Q_{max}) was observed for the nanomaterials compared to the crude samples.

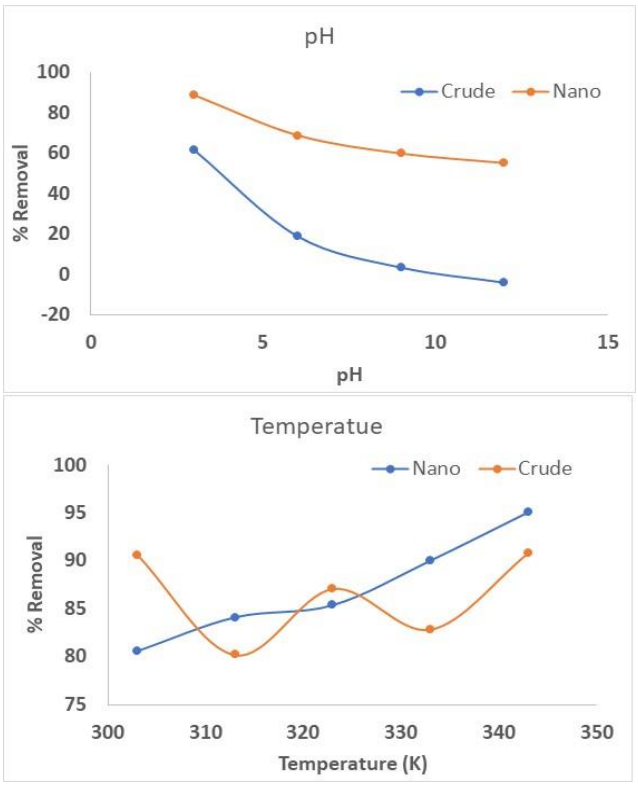

Fig. 3: Variation of percentage amoxicillin removed with pH and temperature

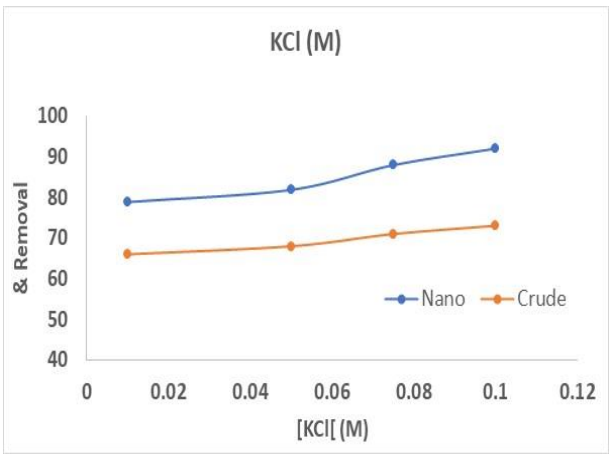

Fig. 4: Variation of percentage amoxicillin removed with ionic strength

The CaONPs (Nano(SN)) gave Q_{maz} of 94760 mg/g while the crude sample (Crude(SN)) showed the lowest (Q_{max} = 7788.16 mg/g). The observed maximum adsorption capacity is larger than the values reported for most CaO-based nanoparticles such as 63 mg/g (Kumar *et al*., 2022), 8.1 mg/g (Oruganti *et al*., 2022) and 225 mg/g (Oladoja *et al*., 2012). The differences can be attributed to several factors. However, in generality, Q_{max} values are known to vary based on the method of synthesis, environmental conditions (such as temperature, pH, amount of adsorbate, the presence of other ions, initial dye concentration, etc.), and the type of adsorbate. The fitness of the slope values indicated lower error for both adsorbents but better for the nanomaterials compared to the crude sample. The sum of square errors and mean square errors are low, indicating the reliability of the Langmuir adsorption model for the investigated adsorbents.

Table 2: Langmuir and Statistical parameters deduced from the Langmuir adsorption isotherm for crude and CaONPs from snail shells

Parameter	CaONPs	Crude
Nano(BN)	**Nano (SN)**	**Crude (SN)**
Slope ± SE	$1.0553 \times 10^{-4} \pm 1.0E-06$	$1.284 \times 10^{-4} \pm 2.2E-06$
Intercept	$8.928 \times 10^{-5} \pm 3.3E-05$	$1262 \times 10^{-4} \pm 8.9E-05$
R^2	0.9990	0.9997
Q_{max} (mg/g)	94760	7788.16
k_L	1.1820	1.0174
SS	0.00001949	0.00002887
MS	0.000019481	0.00002887
SSE	0.00000000198	0.00000003940
MSE	0.000000004921	0.00000000920

****SS = sum of square, MS = mean square, SSE = sum of square error, MSE = mean square error**

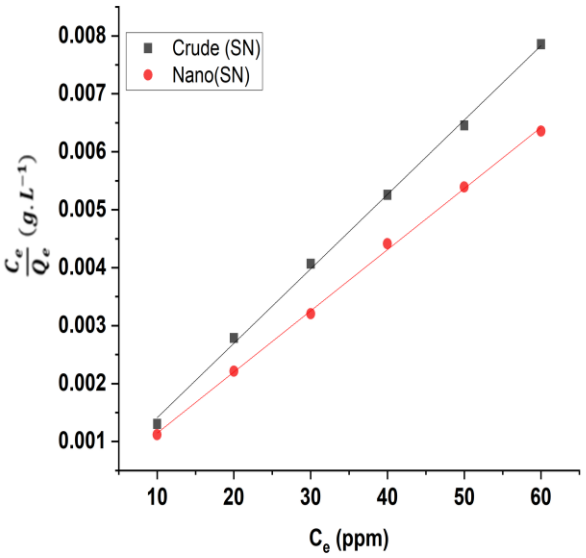

Fig. 5: Variation of $\frac{C_e}{Q_e}$ with C_e for the adsorption of amoxicillin by crude and CaONPs from snail shells according to the Langmuir model

3.4 Thermodynamics of the adsorption

Equation 6 describes the Transition state equation that was used for the evaluation of the enthalpy and entropy changes of the adsorption process through the slope and intercept respectively. (Odoemelam *et al*., 2018)

$$lnk_{eq} = \frac{\Delta S}{R} - \frac{\Delta H}{RT} \quad (6)$$

The equilibrium constant was evaluated as a ratio of the concentration of the drug adsorbed to the equilibrium concentration, that is $k_{eq} = \frac{C_{ads}}{C_e}$, consequently, based on equation 7, a plot of $ln\left(\frac{C_{ads}}{C_e}\right)$ against 1/T (Fig. 6) was employed in the evaluation of the enthalpy (i.e. ΔH = $slope \times R$) and entropy ($\Delta S = intercept \times R$).

$$ln\left(\frac{C_{ads}}{C_e}\right) = \frac{\Delta S}{R} - \frac{\Delta H}{RT} \quad (7)$$

The evaluated values (Table 3) show that the adsorption is exothermic for the nanoparticles but endothermic for the crude materials. The results also reveal higher R^2 values and a lower

sum of square error as well as mean square error for the data representing the nanomaterials than their corresponding precursor (crude). The irregular pattern observed for the crude materials shows the instability of the samples due to temperature changes.

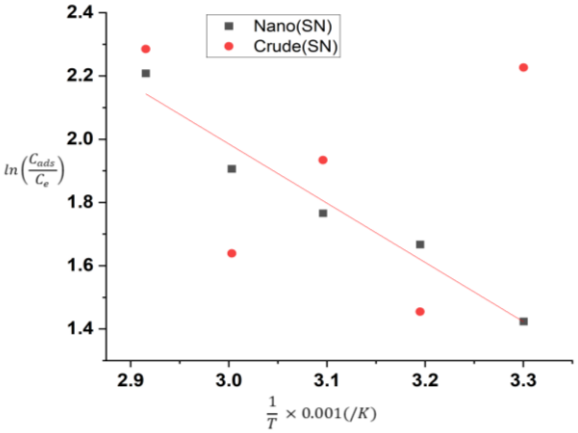

Fig.: 6: Variation of lnk_{eq} ($ln\left(\frac{C_{ads}}{C_e}\right)$ (lnk_{eq}) with 1/T for the adsorption of amoxicillin by Crude(SN) and Nano(SN)

Table: 3: Transition and Statistical parameters for crude (SN) and Nano(SN)

Parameter	Nano (SN)	Crude (SN)
Slope ± SE	-1.87342±0.2191	-0.24612±1.3647
Intercept	7.60532±0.68029	2.67134±4.23736
R^2	0.9606	0.01073
ΔH (J/mol)	-15.0768	-2.0462
ΔS (J/mol)	63.2306	22.2095
SS	0.325	0.00561
MS	0.325	0.00561
SSE	0.01334	0.5174
MSE	0.00445	0.17247

3.5 Kinetic of the adsorption

The test for the best-fitted kinetic models indicated the fitness of the pseudo-second-order, intra-particle diffusion and liquid film diffusion models. The linear form of the pseudo-second-order kinetic is given by equation 8 (Eddy *et al*., 2022a,b)

$$\frac{t}{Q_t} = \frac{1}{k_2 Q_e^2} + \frac{t}{Q_e} \quad (8)$$

Consequently, plots shown in Fig. 7 were developed by graphing values of $\frac{t}{Q_t}$ versus t to obtain slope = $\frac{1}{Q_e}$ and intercept equal to $\frac{1}{k_2 Q_e^2}$. Kinetic parameters deduced from the plots for both Crude (SN) and Nano(SN) are shown in Table 4. It is evident from the recorded values that both adsorbents show good fitness to the pseudo-second-order plots, contrary to their fitness to thermodynamic models. However, the evaluated kinetic constant and the equilibrium amounts of the drug adsorbed are higher for the nanoparticles than the crude materials. Therefore, the kinetic model also confirms that Nano (SN) is a better adsorbent than Crude (SN)

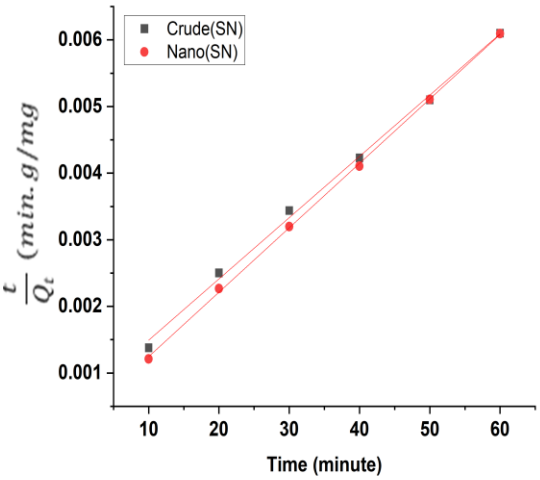

Fig. 7: Pseudo second-order plots for the adsorption of amoxicillin by SN

The kinetics of the intraparticle diffusion model was also investigated, based on equation 9 and therefore showed a linear plot concerning values of Q_t against the square root of the corresponding time, t. (ref). Such plots, covey information on the dominancy of the intraparticle diffusion if the intercept, C is equal to zero, otherwise, film diffusion

(equation 10) may prevail (Garg *et al*., 2022; Odiongenyi and Afangide, 2019)

$$Q_t = k_{int}t^{\frac{1}{2}} + C \quad (9)$$

$$-\ln\left(1 - \left(\frac{Q_t}{Q_e}\right)\right) = k_{LF}t + C \quad (10)$$

From Fig. 8, it is observed that the intraparticle diffusion plot did not give a zero intercept, although R^2 and error variables supported the fitness of the plots that -intercept (Table 5),

Table 4: Pseudo second-order kinetics and statistical parameters for the adsorption of amoxicillin by Crude (SN) and Nano (SN)

Parameter	Nano (SN)	Crude (SN)
Slope ± SE	$9.0672 \times 10^{-5} \pm 9.6895 \times 10^{-7}$	$9.020 \times 10^{-5} \pm 2.3402 \times 10^{-6}$
Intercept	$2.7817 \times 10^{-4} \pm .37734 \times 10^{-5}$	$5.7183 \times 10^{-4} \pm .9114$
R^2	0.9996	0.9974
Q_e (mg/g)	11028.76	11086.47
$k_2(min^{-1})$	3.965×10^{7}	1.9388×10^{-4}
SS	0.0000163696	0.0000148094
MS	0.0000163696	0.0000148094
SSE	0.00000000657199	0.00000003833 58
MSE	0.00000000164 3	0.00000000958 394

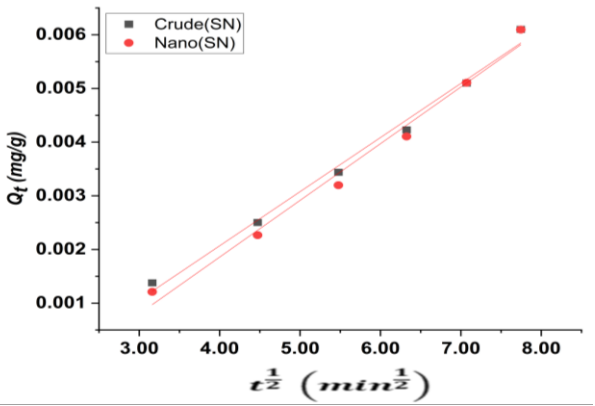

Fig. 8: Intraparticle diffusion plots for the adsorption of amoxicillin by Crude (SN) and Nano (SN)

Table 5: Intraparticle diffusion model (IPD) Liquid film diffusion model (LFD) and statistical parameters deduced from the Pseudo second order plots for Crude (SN) and Nano (SN)

Parameter	Nano(SN)	Crude (SN)
IPD		
Slope ± SE	0.00106±0.00	0.00101±0.00
Intercept	-0.00237±0.000	-0.00197±0.00
R^2	0.9856	0.9903
k_{int} ($/min$)	0.00106±0.0000638 156	0.00101±0.007 15
	-0.00237±0.00	-0.00197±0.00
SS	0.0000161407	0.0000147039
MS	0.0000161407	0.0000147039
SSE	0.000000241	0.00000014
MSE	0.000000059	0.000000036
LFD		
Slope ± SE	0.88091±0.31=2	0.18707±0.40
Intercept	-19.61306±12.88	-3.67524±16.10
R^2	0.7189	0.06873
k_{LF} (/ min)	0.88091±0.31804	0.18707±0.40
C	-19.61306±12.88	-3.6752±16.09
SS	1334.73337	60.19079
MS	1334.7334	60.19079
SSE	521.9394	815.5625
MSE	173.97981	271.85418

Therefore, the liquid film diffusion plots are represented by plots of $-\ln\left(1 - \left(\frac{Q_t}{Q_e}\right)\right)$ versus t (in Fig. 9) was also developed. Parameters deduced from these plots are also presented in Table 5.

Both sets of graphs showed an excellent degree of fitness. However, based on the evaluated rate constant, intraparticle diffusion of the adsorbate unto the adsorbent exerted a greater influence than the liquid film diffusion. The relative contribution of liquid film diffusion seems minimal for both Crude (SN) and Nano (SN) because of the large differences in their respective rate constants. On the contrary, since the intercepts on both plots were not

equal to zero, we conclude that both models have some impact on the diffusion of the amoxicillin molecules before their adsorption.

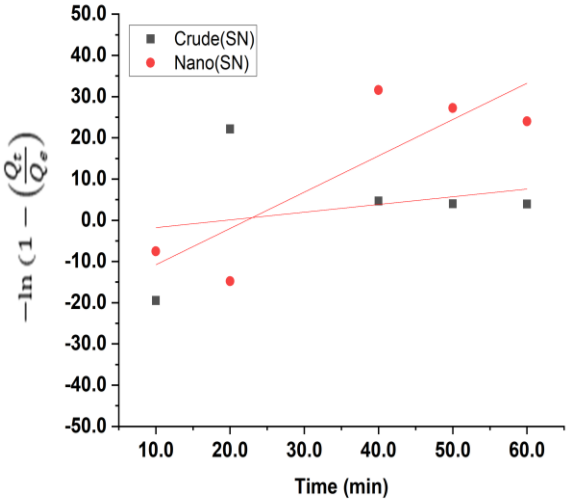

Fig. 8: Liquid film diffusion plots for the adsorption of amoxicillin by Crude (SN) and Nano (SN)

4.0 Conclusion

The findings drawn from the study confirm that snail shell has some inherent adsorption capacity for the removal of amoxicillin contaminants in water. However, due to some surface imperfections, its capacity is limited under certain conditions. The conversion of snail shells to CaONPs through the sol-gel method provides an option for the redefining of new surface properties which presented better surface properties including adsorption removal of amoxicillin from an aqueous solution. The thermodynamic behaviour of the crude snail shell powder as an adsorbent displays a significant instability compared to that of Nano (SN).

5.0 References

Abdelatif, Y., Gaber, A.-A.M., Fouda, A. E. A. S. & Alsoukarry, T. (2020). Evaluation of calcium oxide nanoparticles from industrial waste on the performance of hardened cement pastes: physicochemical study. *Processes 8*, 401. https://doi.org/10.3390/pr8040401.

Abubakar, I. R., Maniruzzaman, K. M., Dano, U. L., AlShihri, F. S., AlShammari, M. S., Ahmed, S. M. S., Al-Gehlani, W. A. G. & Alrawaf, T. I. (2022). Environmental Sustainability Impacts of Solid Waste Management Practices in the Global South. *Int. J. Environ. Res. Public Health* **2022**, *19*, 12717. https://doi.org/10.3390/ijerph191912717

Adedara, M.L., Taiwo, R., & Bork, H.. R. (2023). Municipal solid waste collection and coverage rates in Sub-Saharan African Countries: A comprehensive systematic review and meta-analysis. *Waste, 1*, pp. 389-413. https://doi.org/10.3390/waste1020024.

Bayuseno, A. P., Prasetya, A. I., Ismail, R., Setiyana, B. & Jamari, J. (2022). Reuse of waste crab shells for synthesis of calcium carbonate as a candidate biomaterial. Rasayan J. Chem., 15(1): 523-528(2022) http://dx.doi.org/10.31788/RJC.2022.1516640

Condurache, B. C., Cojocaru, C., Samoila, P., Cosmulescu, S.F., Predeanu, G., Enache, A. C. & Harabagiu, V. (2022). Oxidized biomass and Its Usage as Adsorbent for Removal of Heavy Metal Ions from Aqueous Solutions. Molecules 2022, 27, 6119. https://doi.org/10.3390/molecules27186119.

Eddy, N. O., Garg, R., Garg, R., Aikoye, A. & Ita, B. I. (2022b). Waste to resource recovery: mesoporous adsorbent from orange peel for the removal of trypan blue dye from aqueous solution. *Biomass Conversion and Biorefinery*, DOI: 10.1007/s13399-022-02571-5.

Eddy, N. O., Garg, R., Garg, R., Eze, S. I., Ogoko, E. C., Kelle, H. I., Ukpe, R. A., Ogbodo, R. & Chijoke, F. (2023a). Sol-gel synthesis, computational chemistry, and applications of Cao nanoparticles for the remediation of methyl orange contaminated water. Advances in Nano Research,

https://doi.org/10.12989/anr.2023.15.1.000 .

Eddy, N. O., Odiongenyi, A. O., Garg, R., Ukpe, R. A., Garg, R., El Nemir, A., Ngwu, C. M. & Okop, I. J. (2023b). Quantum and experimental investigation of the application of *Crassostrea gasar* (mangrove oyster) shell–based CaO nanoparticles as adsorbent and photocatalyst for the removal of procaine penicillin from aqueous solution. *Environmental Science and Pollution Research*, doi:10.1007/s11356-023-26868-8.

Eddy, N. O., Odoemelam, S. A., Ogoko, E. C., Ukpe, R. A., Garg, R. & Anand, B. (2022c). Experimental and quantum chemical studies of synergistic enhancement of the corrosion inhibition efficiency of ethanol extract of *Carica papaya* peel for aluminum in solution of HCl. *Results in Chemistry*, 100290, https://doi.org/10.1016/j.rechem.2022.100290. .

Eddy, N. O., Ukpe, R. A., Ameh, P., Ogbodo, R., Garg, R. & Garg, R. (2022a). Theoretical and experimental studies on photocatalytic removal of methylene blue (MetB) from aqueous solution using oyster shell synthesized CaO nanoparticles (CaONP-O*). Environmental Science and Pollution Research*, https://doi.org/10.1007/s11356-022-22747-w.

Garg, R., Garg, R., Eddy, N. O., Almohana, A. I., Fahad, S., Khan, M. A. & Hong, S. H. (2022). Biosynthesized silica-based zinc oxide nanocomposites for the sequestration of heavy metal ions from aqueous solutions. *Journal of King Saud University-*Science https://doi.org/10.1016/j.jksus.2022.101996.

Habte, L., Shiferaw, N., Mulatu, D., Thenepalli, T., Chilakala, R. & Ahn, J. W. (2019). Synthesis of nano-calcium oxide from waste eggshell by sol-gel method. *Sustainability, 11*, 3196. https://doi.org/10.3390/su11113196.

Hamester, M. R. R., Santos, P. & Becker, B. D. (2012). Characterization of calcium carbonate obtained from oyster and mussel shells and incorporation in polypropylene. Materials Research, 15 (2), https://doi.org/10.1590/S1516-14392012005000014

Jadhav, V. R., Bhagare, A. M., Lokhande, D. D., Vaidya, C., Dhayagude, A., Khalid, M., Aher, J., Mezni, A. & Dutta, M. (2022). Green synthesized calcium oxide nanoparticles (CaO NPs) using leaves aqueous extract of *Moringa oleifera* and evaluation of their antibacterial activities. *Journal of Nanomaterials,* 2, pp. 1-7, doi:10.1155/2022/9047507.

Jalu, R. G., Chamada, T. A. & Kasirajan, R. (2021). Calcium oxide nanoparticles synthesis from hen eggshells for removal of lead (Pb(II)) from aqueous solution. *Environmental Challenges*, 4, https://doi.org/10.1016/j.envc.2021.100193.

Kasirajan, R., Bekele, A. & Girma, E. (2022). Adsorption of lead (Pb-II) using CaO-NPs synthesized by solgel process from hen eggshell: Response surface methodology for modeling, optimization and kinetic studies, South African Journal of Chemical Engineering, 40, pp. 209-229, https://doi.org/10.1016/j.sajce.2022.03.008 .Khine, E.E., Koncz-Horvath, D., Kristaly, F. *et al* (2022). Synthesis and characterization of calcium oxide nanoparticles for CO_2 capture. *J Nanopart Res* 24, 139, https://doi.org/10.1007/s11051-022-05518-z/

Khine, E.E., Koncz-Horvath, D., Kristaly, F. *et al*. (2022). Synthesis and characterization of calcium oxide nanoparticles for CO_2 capture. *J Nanopart Res*. 24, 139,

https://doi.org/10.1007/s11051-022-05518-z.

Kofoworola, O. F. (2007). Recovery and recycling practices in municipal solid waste management in Lagos, *Nigeria. Waste Management*, 27, 9, pp.1139-1143, ttps://doi.org/10.1016/j.wasman.2006.05.006.

Kumar JA, Krithiga T, Narendrakumar G, Prakash P, Balasankar K, Sathish S, Prabu D, Pushkala DP, Marraiki, N., Ramu A. G. & Choi D. (2022). Effect of Ca^{2+} ions on naphthalene adsorption/desorption onto calcium oxide nanoparticle: Adsorption isotherm, kinetics and regeneration studies. Environ Res., 112070, doi: 10.1016/j.envres.2021.112070.

Mostafa, F. A., Gad, A. N., Gaber, A. A. M. *et al.* (2022). Preparation, Characterization and application of calcium oxide nanoparticles from waste carbonation mud in clarification of raw sugar melt. *Sugar Technology*, https://doi.org/10.1007/s12355-022-01150-2.

Mostafa, F.A., Gad, A.N., Gaber, AA.M. *et al.* (2023). Preparation, characterization and application of calcium oxide nanoparticles from waste carbonation mud in clarification of raw sugar Melt. *Sugar Tech*., 25, pp. 331–338, https://doi.org/10.1007/s12355-022-01150-2.

Ngouoko, J. J. K., Tajeu, K. Y., Fotsop, C. G., Tamo, A. K., Doungmo, G., Temgoua, R.C.T., Kamgaing, T.& Tonle, I. K. (2022). Calcium carbonate originating from snail ,s for synthesis of hydroxyapatite/l-lysine composite: characterization and application to the electroanalysis of Toluidine Blue. *Crystals*, *12*, 1189. https://doi.org/10.3390/cryst12091189.

Novo, L. B., Gomes da Silva, F. A. N., Bertolino, L. C. & Yokoyama, L. (2022). Amoxicillin Trihydrate Characterization and investigative adsorption using a Brazilian montmorillonite. *Revista Mteria*, 27, 3, DOI: https://doi.org/10.1590/1517-7076-RMAT-2022-0109.

Odiongenyi, A. O. (2010). Utilization of *Musa cecropiodesi* woood saw dust for the removal of dispersed yellow (DY) dye from aqueous solution. *Communication in Physical Sciences, 5, 3, pp.* 270-280.

Odiongenyi, A. O. (2019). Removal of ethyl violet dye from aqueous solution by graphite dust and nano graphene oxide synthesized from graphite dust. *Communication in Physical Sciences*, 4, 2, pp. 103-109.

Odiongenyi, A. O. (2022). Influence of sol gel conversion on the adsorption capacity of crab shell for the removal of crystal violet from aqueous solution. C*ommunication in Physical Science*, 8, 1, pp. 121-127.

Odiongenyi, A. O. and Afangide, N. R.. (2019). Adsorption and thermodynamic studies on the removal of congo red dye from aqueous solution by alumina and nano-alumina. *Communication in Physical Sciences*, 4, 1, pp. 1-7.

Odiongenyi, A. O., Essien, U. I., Ukpong, E. J. & Ekwere, I. O. (2023). Adsorption efficiency of scotch bonnet shells as a precursor for calcium oxide nanoparticles and an adsorbent for the removal of amoxicillin from aqueous solution. *Communication in Physical Sciences*, 9, 3, pp. 367-382.

Odoemelam, S. A., Oji, E. O., Eddy, N. O., Garg, R., Garg, R., Islam, S., Khan, M. A., Khan, N. A. & Zahmatkesh, S. (2023). Zinc oxide nanoparticles adsorb emerging pollutants (glyphosate pesticide) from aqueous solution. *Environmental Monitoring and Assessment*, https://doi.org/10.1007/s10661-023-11255-0.

Ogoko, E. C., Kelle, H. I., Akintola, O. & Eddy, N. O. (2023). Experimental and theoretical investigation

of *Crassostrea* gigas (gigas) shells based CaO nanoparticles as a photocatalyst for the degradation of bromocresol green dye (BCGD) in an aqueous solution. *Biomass Conversion and Biorefinery*. https://doi.org/10.1007/s13399-023-03742-8

Oladoja, N. A., Ojolade, I. A>, Olaseni, S. E., Olatujoye, V. O., Jegede, O. S. & Agunloye, A. O. (2012). Synthesis of nano calcium oxide from a gastropod shell and the performance evaluation for Cr (VI) removal from aqua system. *Industrial & Engineering Chemistry Research 51* , 2, pp. 639-648, DOI: 10.1021/ie201189z.

Oruganti, R.K., Pal, D., Panda, T.K. *et al.* (2022). Green synthesis of calcium oxide nanoparticles impregnated activated carbon from algal–bacterial activated sludge: its application in ciprofloxacin removal. *Int. J. Environ. Sci. Technol.*, https://doi.org/10.1007/s13762-022-04662-2.

Parveen, S., Chakraborty, A., Chanda, D., Pramanik, C. S., Barik, A. & Aditya, G. (2020). Microstructure analysis and chemical and mechanical characterization of the shells of three freshwater snails. *ACS Omega*, *5*, *40*, *pp.* 25757-25771, DOI: 10.1021/acsomega.0c03064.

Toamah, W. O. & Fadhil, A. K. (2019). Preparation of nanoparticles from CaO and use it for removal of chromium (II), and mercury (II) from aqueous solutions. IOP Conf. Series: *Journal of Physics: Conf. Series* 1234, 012086, doi:10.1088/1742-6596/1234/1/012086.

Zargar, T. I., Alam, P., Khan, A. H., Alam, S. S., Abutaleb, A., Hasan, M. A. & Khan, N. A. (2023). Characterization of municipal solid waste: Measures towards management strategies using statistical analysis. *Journal of Environmental Management*, 342, https://doi.org/10.1016/j.jenvman.2023.118331.

Zuliantoni, Z., Suprapto, W., Setyarini, P. H. & Gapsari, F. (2022). Extraction and characterization of snail shell waste hydroxyapatite. Results in Engineering, 14, https://doi.org/10.1016/j.rineng.2022.100390.

Data availability

All data used in this study will be readily available to the public.

Consent for publication

Not Applicable

Availability of data and materials

The publisher has the right to make the data Public.

Competing interests

The authors declared no conflict of interest.

Funding

The authors declared no source of funding

Authors' contributions

AOO designe the work. UIE, CO and IE participated in the bench work while the first and final draft was written by UIE and supervised by AOO.